

## Durham Research Online

---

### Deposited in DRO:

14 December 2015

### Version of attached file:

Accepted Version

### Peer-review status of attached file:

Peer-reviewed

### Citation for published item:

Aguilar, Juan A. and Kenwright, Simon J. (2016) 'Robust NMR water signal suppression for demanding analytical applications.', *Analyst.*, 141 (1). pp. 236-242.

### Further information on publisher's website:

<http://dx.doi.org/10.1039/C5AN02121A>

### Publisher's copyright statement:

### Additional information:

---

### Use policy

The full-text may be used and/or reproduced, and given to third parties in any format or medium, without prior permission or charge, for personal research or study, educational, or not-for-profit purposes provided that:

- a full bibliographic reference is made to the original source
- a [link](#) is made to the metadata record in DRO
- the full-text is not changed in any way

The full-text must not be sold in any format or medium without the formal permission of the copyright holders.

Please consult the [full DRO policy](#) for further details.

# Robust NMR water signal suppression for demanding analytical applications

Received 00th January 20xx,  
Accepted 00th January 20xx

DOI: 10.1039/x0xx00000x

www.rsc.org/

Juan A. Aguilar<sup>\*a</sup> and Simon. J. Kenwright<sup>a, b</sup>

We describe the design and application of robust, general-purpose water signal suppression pulse sequences well suited to chemometric work. Such pulse sequences need to deal well with pulse mis-calibrations, radiation damping, chemical exchange, and the presence of sample inhomogeneities, as well as with significant variations in sample characteristics such as pH, ionic strength, relaxation characteristics and molecular weight. Of course, such pulse sequences should produce undistorted lineshapes and baselines and work well both under automation and in the hands of non-experts. As an example, one such pulse sequences, *Robust-5*, will be presented. This new pulse sequence meets those criteria and is able to reduce a 50 M proteo water signal down to a 0.9 mM level, without fine tuning, and under automation, and it is therefore well suited to the most demanding of analytical applications.

## 1 Introduction

Suppression of strong solvent signals in NMR is a necessity for the analysis of samples with a high proteo water content. There are a number of pulse sequences that achieve this.<sup>1,2</sup> Many will produce good results in the hands of specialists, particularly when there is sufficient time to optimize conditions on individual samples. However, the scenario where specialists work optimizing experiments on a sample-by-sample basis is increasingly rare. Samples are often run under automation and, at times, manually by researchers. Unfortunately, the multidisciplinary character of many projects means that the time allocated to learn NMR is often insufficient to allow every researcher to become an expert. For these reasons, it is important to design robust, easy to set up, and efficient pulse sequences that are tolerant of the problems that challenge even the experts. An ideal general-purpose pulse sequence should deal well with pulse mis-calibrations, radiation damping, chemical exchange, the presence of sample inhomogeneities, and significant variations in sample characteristics such as pH, ionic strength, relaxation characteristics, and molecular weight. Of course, such pulse sequences should produce undistorted line shapes and baselines, and work well under automation. The present paper deals with the design of one such pulse sequence, the *Robust-5*, but the principles discussed here could be used to design other pulse sequences. As such, these principles are as

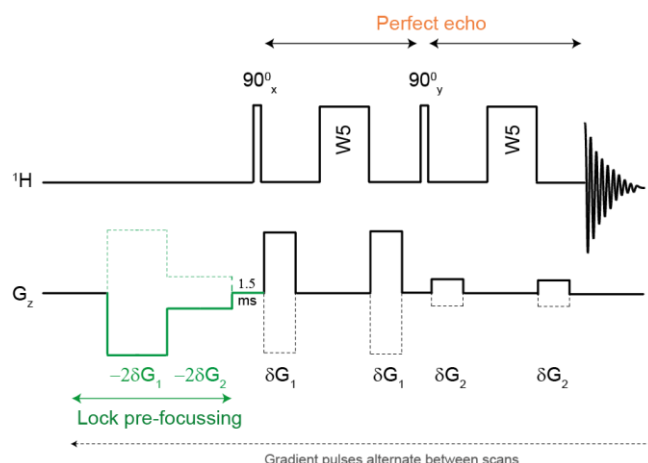


**Fig. 1.** The *Robust-5* pulse sequence. Eddy current distortions as well as lock signal destruction are minimised using lock pre-focussing pulsed field gradients. J-evolution distortions are minimised using a "perfect echo" approach. Signals from parts of the sample where  $B_1$  is quite inhomogeneous are eliminated by the phase-cycle. The pulse sequence and its phase cycle can be found in the supplementary information section. The polarity of the gradients alternates between scans. Optimum results can be obtained using  $G_1/G_2 = 5.8$ ,  $G_1 = 28.3$  G cm<sup>-1</sup> and  $\delta = 1.0$  ms. Gradient stabilization delays of 0.5 to 1.0 ms were used.

important as the pulse sequence itself. Particular attention has been paid to addressing problems important for chemometric work.

## 2 Experimental section

The *Robust-5* pulse sequence is presented in Figure 1. Its performance was tested using 400, 600 and 700 MHz spectrometers, with statistical analysis being carried out using the 600 MHz and the 700 MHz spectrometers equipped with *Agilent OneNMR Probes* able to deliver a maximum pulsed

<sup>a</sup> Department of Chemistry, Durham University, South Road, Durham, DH1 3LE (UK). J.a.aguilar@durham.ac.uk

<sup>b</sup> Current address: The Queen's College, University of Oxford, Ox1 4AW (UK).

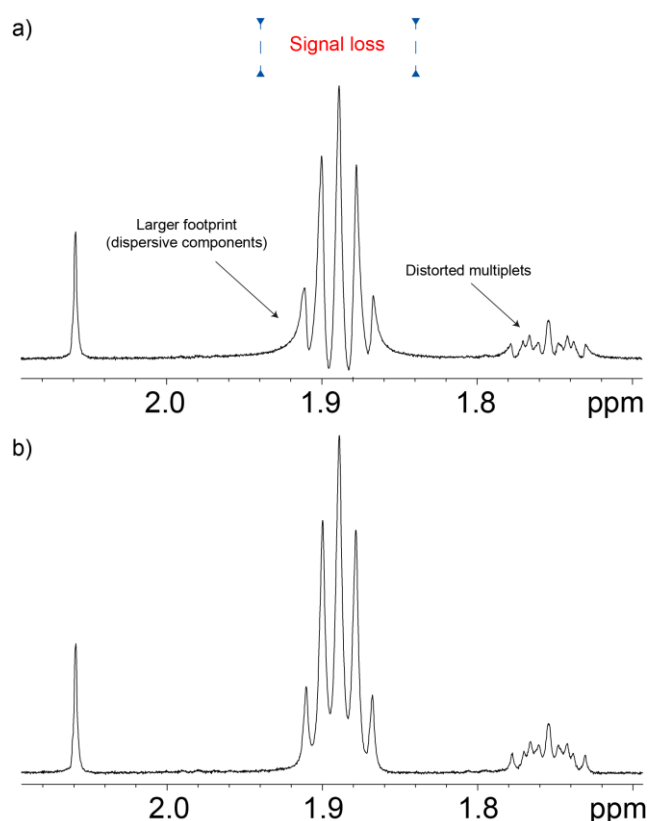


**Fig. 2.** Excitation sculpting pulse sequences produce signals that are distorted due to J-modulation. Such modulations reduce signal intensities, distort multiplets, and increase signal overlap due to the presence of dispersive components. In (a), where the classic W5-based excitation sculpting pulse sequence has been used, these problems are readily apparent. In (b) these problems have been eliminated using the new *Robust-5* pulse sequence. See text for details. The sample is  $\gamma$ -aminobutyric acid (GABA) dissolved in 90 %  $\text{H}_2\text{O}$ -10 %  $\text{D}_2\text{O}$ .

field gradient of  $62 \text{ G cm}^{-1}$ . Thirty two scans were collected each comprising 65536 complex data points and a spectral width of 10 KHz. The repetition time was 6.3 s, of which 3.3 comprised the acquisition time. The W5 inter-pulse delay was set to 240  $\mu\text{s}$  when using the 600 MHz spectrometer, and to 287  $\mu\text{s}$  when using the 700 MHz one. In all cases rectangular 1 ms pulsed field gradients were used with a strength of  $G_1=28.3 \text{ G cm}^{-1}$  (first pair) and  $G_2=4.9 \text{ G cm}^{-1}$  (second pair). The gradient stabilization delay was 0.5 ms. The first pair of lock pre-focusing field gradients were separated by 1.5 ms delay from the first radio-frequency pulse. In all cases the timing of the W5 element was time corrected as prescribed by Wang *et al.*<sup>3</sup> To test the performance of the pulse sequence and the degree of suppression that can be achieved under automation, 26 samples were produced covering different sample compositions, concentrations, dynamic ranges, pH, and salinity. The samples were of commercial origin apart from the saliva and the urine ones, which were obtained from a healthy volunteer and used without alteration apart from adding  $\text{D}_2\text{O}$  to a level of 10 % v/v. These samples comprised egg white, river water, fermented soybean paste, dried tuna flakes, tuna-based flavouring, tomatoes, kelp, hand-wash, cayenne pepper, tooth paste (brand 1), tooth paste (brand 2), melt water from

a commercial batch of frozen boiled prawns, boiled prawns (meat), yogurt, grapes, balsamic vinegar, fresh mint leaves, fresh parsley, fresh sage, tomato juice (commercial), garlic cloves, garden peas, and garden pea pods. Those samples that already had a high water content were used without modification other than adding  $\text{D}_2\text{O}$  (10 % v/v) and 3-(trimethylsilyl)-2,2',3,3'-tetraadeuteriopropionic acid (TSP- $\text{d}_4$ ) at 10 mM concentration. In the case of vegetable-based solid samples, 100 mg of material was frozen in liquid nitrogen and crushed using a mortar and pestle, then allowed to thaw. The resultant paste was extracted using 2 mL of  $\text{H}_2\text{O}/\text{D}_2\text{O}$  (90 %, 10 %) containing TSP- $\text{d}_4$  at 10 mM concentration. The sample used in Figure 2 was produced by dissolving 10 mg of  $\gamma$ -aminobutyric acid (GABA) in 90 %  $\text{H}_2\text{O}$ -10 %  $\text{D}_2\text{O}$ .

### 3 Results and discussion

#### 3.1 The basis of the new pulse sequence.

One of the most efficient and widespread solvent signal suppression approaches, and the one used in the present publication, combines selective refocusing pulses with pulsed field gradients. Pulse sequences of this type have the advantage that they do not cause sample heating, attenuate protein signals, cause metabolite protein-mediated saturations or suppress signals from exchangeable protons, all of which are common problems with otherwise robust saturation-based approaches. These pulse sequences are very popular and have been used in fields such as food analysis,<sup>4</sup> metabo(l/n)omics,<sup>5,6</sup> drug discovery,<sup>7</sup> and environmental studies.<sup>8</sup> Within this class, sequences that use the excitation sculpting principle<sup>9</sup> are particularly efficient. Some excitation sculpting pulse sequences use a combination of hard pulses and delays, such as W5,<sup>10</sup> or PM,<sup>11</sup> others a combination of hard and soft pulses.<sup>9,12,13</sup> In the present work, a W5-based approach has been used as a starting point because it can be readily set-up by non-experts and because it lends itself well to the purposes of the present investigation. Starting with the basic W5-based pulse sequence, several elements will be progressively incorporated, although it has to be noted that improving the W5 sequence itself is not the purpose of the present publication, and that the principles discussed here can be equally well applied to the design of other pulse sequences. Although the sequences described here were primarily acquired on Varian equipment, the principles discussed can be readily implemented on any modern spectrometer, and could equally be applied to improve pulse sequences intended to suppress multiple resonances.<sup>14,15</sup>

#### 3.2 The J-modulation problem.

Apart from the excitation sculpting principle itself, a particular feature that makes this class of pulse sequences efficient is that the suppression block is located just before the acquisition period, so there is little opportunity for the water signal to recover. This feature is particularly useful when adding such schemes to other pulse sequences but, unfortunately, it comes at a price since signals evolve

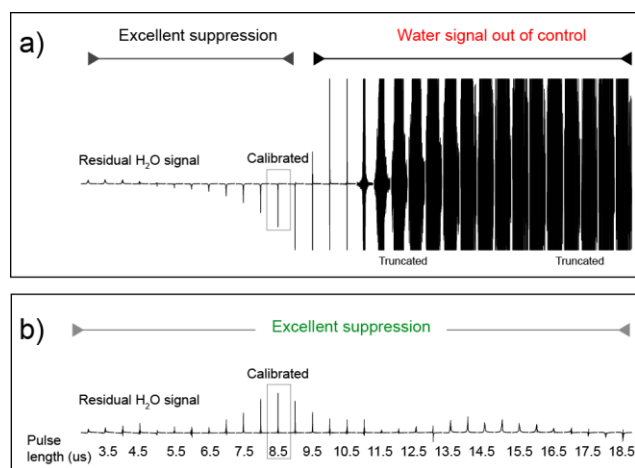


**Fig. 3.** Plots of the residual water signal as a function of pulse length for the classic W5 pulse sequence (a) and for the new *Robust-5* (b). The value plotted represents the value of first pulse in the pulse sequence, ideally a hard  $\pi/2$  pulse. All pulses in the pulse sequence are calculated with respect to this value so that all pulses are proportionally mis-set when this one is. The performance of both versions is excellent when pulses of the correct length, or lower, are used. However, longer pulses (b) cause the classic version to lose control of the water signal. The result is an unusable spectrum, as can be seen in Figure 4a. The same result was obtained when shaped pulses were used instead of the W5 composite. In stark contrast, the performance of *Robust-5*, Figures 3b and 4b, is always excellent. The sample is an aqueous extract of a dried tuna food supplement. Details of its preparation are reported in the experimental section.

according to their J-couplings during the excitation sculpting period. This distorts and weakens signals, and even increases signal overlap,<sup>16</sup> causing problems for chemometric work. For example, distorted signals impair the use of pattern recognition programs. Often these distortions feature negative components that interfere with non-negativity constraints used in procedures such as automated baseline corrections, and multivariate analysis. These distortions can be seen in Figure 2. Note that this problem is not exclusive to the W5-based pulse sequences, but is common among the Watergate family. The problem is always present although it is usually overlooked. Such is the case when signals overlap, as in metabo(l/n)omic samples, or when signals are broadened either by the use of apodisation or simply by their relaxation processes. The use of bucketing, typical of multivariate statistics such as principal component analysis (PCA), might conceal the problem in early stages of the analysis, but it will reappear while trying to identify the species that form the principal components.

As described, J-evolution increases signal overlap because it converts in-phase signals into anti-phase ones, which having a dispersive character, occupy more than four times the spectral width of the corresponding in-phase signal. Fortunately the in-phase signal usually dominates. Furthermore, the presence of anti-phase components causes quantitation errors since typical anti-phase signals have zero net integral.

Another undesirable consequence of the modulation problem is that it prevents users from realizing the full potential of these sequences because the length of the pulsed

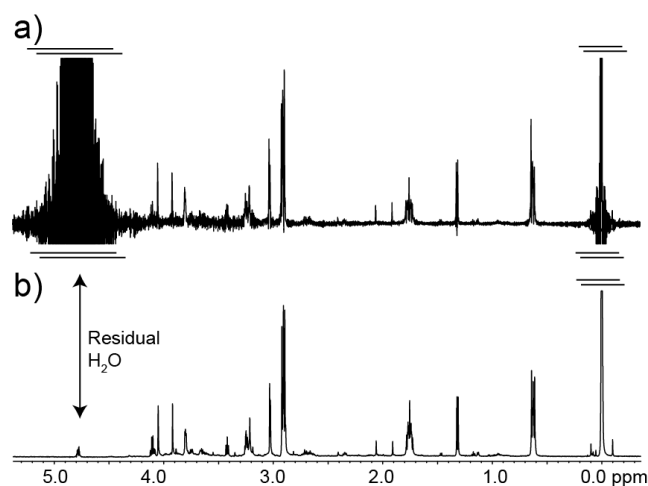


**Fig. 4.** The classic excitation sculpting-W5 pulse sequence fails when pulses longer than the correct ones are used (a). In stark contrast, the descendant of the W5 pulse sequence, *Robust-5* does not fail even when pulses are 50 % longer than they should be (b). This tolerance to pulse mis-calibration makes the new pulse sequence ideal for automation as well as for manual NMR experiments carried out by non-experts. The sample is the same presented in Figure 3 and both spectra correspond to the case where a 12.5  $\mu$ s pulse was used instead of the correct 8.5  $\mu$ s one. As in Figure 3, all pulses in the pulse sequence were calculated with respect to this one as if it were a  $\pi/2$  pulse. All other experimental details have been specified in the experimental section.

gradients and the associated gradient recovery delays have to be kept short in order to avoid large distortions. The consequence of short pulsed field gradients is a larger unsuppressed water signal, while reduced gradient recovery delays cause field disturbances that result in further distortions, see Figures 5 and 6, and the accompanying text.

In principle, some anti-phase components can be removed using a purging spin-lock, but while this eliminates the dispersive component of the signal, it sometimes does so at the cost of degrading the quality of the suppression. Fortunately, there are better solutions. The anti-phase terms can be mostly reconverted into in-phase terms using the so called “perfect echo”.<sup>17,18</sup> This can be achieved by adding a 90° pulse with a phase orthogonal to that of the excitation pulse in between the two refocusing elements, so as to form two echoes, as in Figure 1. The refocusing element can be the W5 composite pulse, as in Figure 1, or any other suitable refocusing element provided that it does not produce major phase shifts. The improvements in the quality of the data can be appreciated comparing the results of the classic W5, itself a good pulse sequence, with those produced by the new *Robust-5* sequence that incorporates the “perfect echo”. See Figure 2. Multiplets in the former show dispersive character, larger footprints, and, overall, reduced intensities when compared with the latter. A further benefit of the latter, is that both gradient duration and recovery times can be lengthened to produce better suppression factors, and to reduce field disturbances. These two factors are described in detail below.

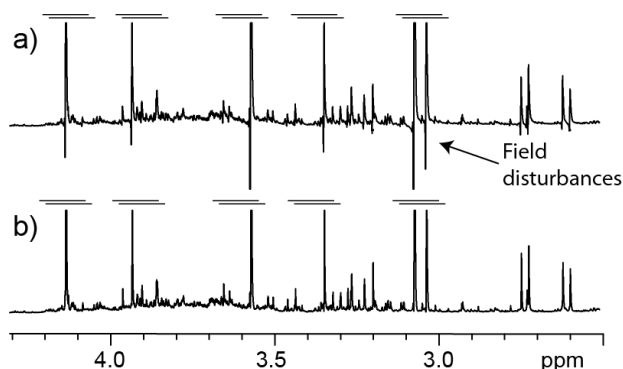


**Fig. 5.** Signal distortions caused by the switching of the field gradient coil are common artefacts from pulse sequences that use pulsed field gradients. These are evident in (a) where a classic W5-based excitation sculpting pulse sequence has been used. Note that these distortions cannot be eliminated with phase corrections. The problem is absent in (b), where pre-focussing pulsed field gradients have been used in the *Robust-5* sequence. The gradient stabilization delay was 0.5 ms in both cases.

### 3.3 Tolerance to mis-calibrations and radiation damping.

A necessary quality of any robust pulse sequence is its tolerance to pulse mis-calibrations, which are more common on real samples than we might wish, particularly under automation. Both the *Robust-5* and the classic W5-based excitation sculpting pulse sequences were the subject of several tests in which all the radiofrequency pulses were mis-calibrated. Radiation damping was always present in these tests, as expected at high fields when dealing with samples dissolved in 90 % H<sub>2</sub>O. The results are seen in Figures 3 and 4. While the classic version fails to attenuate the water signal when pulses are longer than they should be, see Figure 3, *Robust-5* remains always reliable. While, in the first case mis-calibration results in unusable spectra (Figure 4a) in the second one the results are still fine (Figure 4b). It was also found (results not shown) that the excitation sculpting pulse sequence that uses shaped pulses instead of the W5 element also fails when pulses are longer than they should be.

### 3.4 Signal distortions due to field disturbances.

A typical problem of pulse sequences that use pulsed field gradients is that the gradients can cause signal and baseline distortions.<sup>19</sup> Field gradients destroy the deuterium signal used by the field-frequency feedback mechanism that keeps signals from drifting when the main magnetic field drifts ("the lock"). An additional problem derived from the use of pulsed field gradients is that the switching of the gradient coil generates eddy currents. These introduce field disturbances that cause further distortions that often make signals look tilted towards one side, giving the false impression that there is a phasing problem. See Figures 5 and 6. Notice, however,

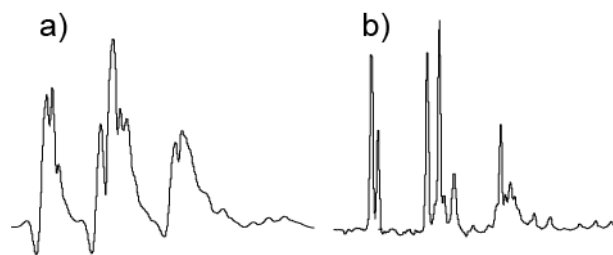


**Fig. 6.** In (a) signals from a saliva sample show distortions caused by the switching of the gradient coil). Note that these cannot be corrected using phase corrections. In (b) reference deconvolution has been used to simultaneously correct these as well as to achieve an improvement in resolution. Note that the signals in b) are narrower than in a). Note also that pre-focussing and reference deconvolution can be used together.

that the problem cannot be removed by phase corrections. The severity of the eddy current problem depends on a number of factors. In our NMR service, two probe-heads running on 400 and 600 MHz spectrometers show moderate effects; another one, operating on the same 600 MHz instrument, is mostly problem-free, while the probe-head of our 700 MHz instrument shows intrusive distortions intermittently.

While problems with eddy currents can be minimized by increasing gradient stabilization delays, there is a conflicting demand to keep gradient stabilization delays short to minimize the J-evolution problem. With the "perfect echo" approach, however, they can be lengthened appropriately. At the same time, the destruction (defocusing) of the deuterium signal can be mostly reversed by using lock pre-focusing pulsed field gradients with the same area but the opposite polarity as those already present in the pulse sequence.<sup>20</sup> These pre-focusing elements should be located before the first excitation pulse to avoid destroying signals of interest, as shown in Figure 1. This only works when pairs of positive and negative gradients are close to one another relative to T<sub>2</sub>, otherwise lock signals decay before they can be refocused. Using this approach, the loss in lock signal is as low as 10 %. This should enable spectrometers to maintain better control of the feedback mechanism, and to prevent an irreversible loss of the lock when dealing with samples, such as the present ones, that have a low deuterium content. See Figure 7.

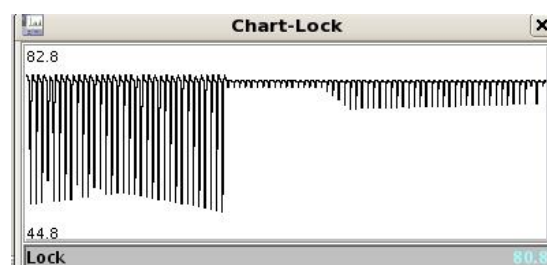


**Fig. 7.** A screen capture of the time course of the lock signal level. On the left, the lock signal drops due to the use of the simple pulsed field gradients. On the right this has been minimised by the use of pre-focusing pulsed field gradients as described in the text.

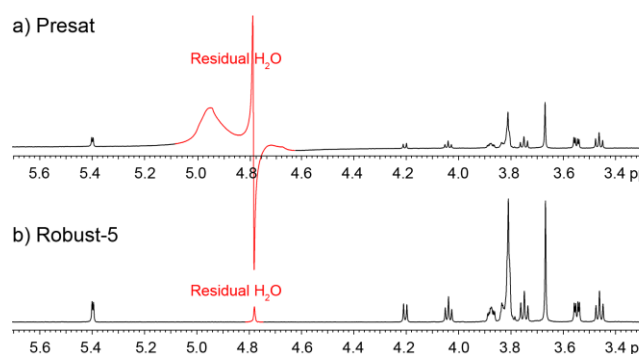


**Fig. 8.** Signals from very inhomogeneous parts of the sample (located at the edges of the sample) are often intrusive as can be seen in (a) where a strong saturation pulse (180 Hz, 3s) was used to attenuate the water signal. Good suppression of these elements is, however, easily accomplished using *Robust-5* (b). Both spectra were run under the same conditions, as described in the experimental section. The sample is a commercial test sample commonly used to test the performance of water signal suppression. It contains sucrose (2 mM),  $\text{NaN}_3$  (2 mM) and DSS (fully deuterated 4,4-dimethyl-4-sylapentane-1-sulfonic acid, 0.5 mM) in 90 %  $\text{H}_2\text{O}/10\%$   $\text{D}_2\text{O}$  v/v.

Another benefit of the pre-focusing approach is that it reduces the severity of the eddy current problem because every gradient pulse has an equivalent one with the opposite polarity.<sup>21</sup> Finally, a judicious arrangement of the pulsed field gradients can be used to further minimize the problem. The closer the gradient pulses are to the beginning of the FID, the larger the distortion they cause; the stronger they are, the worse. It makes sense then to make the pair closer to the beginning of the FID the weaker pair, and those further from the FID the stronger, as in Figure 1. This also makes sense because the last pair has to deal with a water signal that has been reduced to a fraction of its original size by the first pair. The efficiency of the approach in reducing distortions caused by eddy currents can be appreciated in Figure 5.

Another approach that can be used to correct signal distortions due to field disturbances is reference deconvolution.<sup>22</sup> This approach uses a signal of known characteristics, typically a singlet such as TSP, to eliminate experimental infelicities such as imperfect shimming, spinning sidebands and, of course, signal distortions due to field disturbances. Its application is very simple and it can be used to produce good results out of otherwise unusable spectra. Worth noting is the potential of reference deconvolution in improving the quality of data in metabo(l/n)omic studies, a field that often requires the suppression of strong water signals.<sup>23</sup> In Figure 6, for example, reference deconvolution was used to correct signal distortions due to field disturbances as well as to maximize the resolution of the spectrum (resolution enhancement). It has to be kept in mind though, that while reference deconvolution can correct problems caused by eddy currents, it cannot avoid the destruction of the deuterium signal, so the use of the pre-focusing gradients is still recommended, although both techniques can be profitably used together.

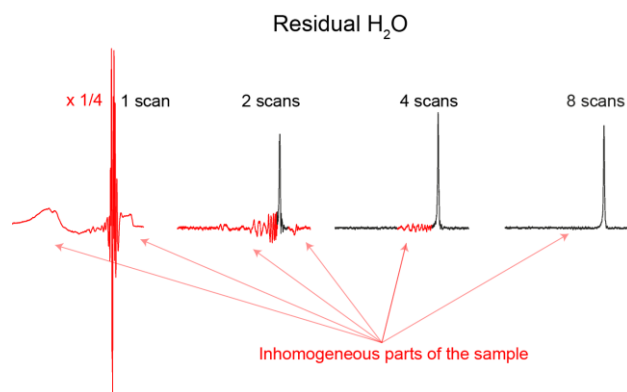


**Fig. 9.** Water signals from inhomogeneous parts of the sample located at the edges of the sample, corresponding here to the red lobes around the sharp water peak, are suppressed by the phase cycle of *Robust-5*. This phase cycle, see the supplementary information, acts as a “depth-pulse”, see text for details. The figure plots the residual water signal as a function of the number of scans. It can be seen that eight scans give clean results although the full phase cycle requires thirty two. In any case, the number of scans used must be a multiple of two. The sample used is the same as in Figure 8. The first spectrum has been reduced vertically by a factor of four to fit it in the figure.

Again it should be noted that problems caused by the use of pulsed field gradients are not exclusive to the type of pulse sequence used here.

### 3.5 Suppression of signals from very inhomogeneous parts of the sample.

A remarkable feature of *Robust-5*, and possibly of all the excitation sculpting family, is that it eliminates signals from regions where  $B_1$  is inhomogeneous such as regions close to the top and bottom of the coil.<sup>24</sup> Such signals are problematic and often limit otherwise good pulse sequences such as pre-saturation. An example of the problem while using pre-saturation can be seen in Figure 8. Notice the broad components of the residual water signal. These remain unsuppressed even when using such a powerful saturation pulse that many real sample signals are also attenuated. The lower the concentration of the sample, the more intrusive these signals are. These signals can be eliminated by adding “depth pulses”,<sup>25</sup> but even this is unnecessary in the case of *Robust-5*, as the phase cycle of the W5 elements will have the same effect, *i.e.*, it will eliminate magnetisation arising from parts of the sample with poor  $B_1$  homogeneity, as show in Figures 8 and 9. Clean results can be produced provided that at least eight transients are used, although thirty two are preferred to complete the pulse sequence phase cycle. In any case, the number of transients should be always a multiple of two, as shown in Figure 9.

### 3.5 Robustness of the pulse sequence under automation.

Finally, the performance of the new pulse sequence was tested under automation using 26 samples and several spectrometers. These samples were also used to determine



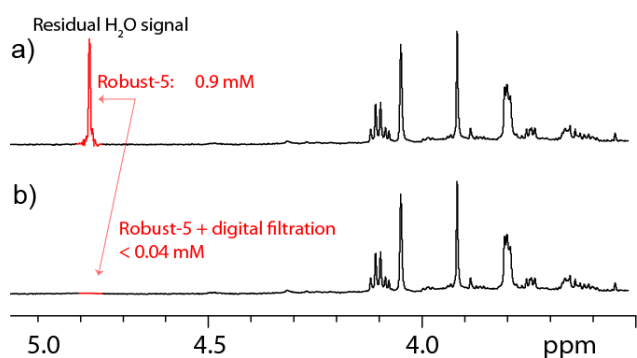


**Fig. 10.** Robust-5 spectra of an aqueous extract of a tuna-based food product. The sample ran under automation and without particular optimizations. The residual water signal (a) was reduced from a 50 M to a 0.9 mM level. The quality of the suppression is such that it allows the use of automatable digital filters to achieve near perfect suppression, i.e. less than 0.04 mM, without baseline distortions, as in (b). See text for details.

whether the new pulse sequence tolerates the presence of radiation damping, a hurdle at high fields,<sup>26</sup> pulse mis-calibrations, and sample inhomogeneities, among other factors. Samples included plant extracts, products from the food and cosmetic industry, several biofluids, river water, and samples from synthetic chemistry. Factors such as pH, and ionic strength varied markedly among the samples. Concentrations ranged over more than an order of magnitude. Pulses were not calibrated on individual samples and radiation damping was always present. Furthermore, some samples developed precipitates, floculates and even bubbles while waiting to be measured. In spite of all of these problems, the pulse sequence performed to a high standard. On average, the residual water signal was reduced to a mere 0.9 mM. Near total suppression (< 0.04 mM) can be achieved using simple processing digital filters in conjunction with *Robust-5*. See Figure 10. As a reference, the concentration of the twelve most abundant human serum metabolites detectable by NMR range from 5 mM (cholesterol) to 0.35 mM ((R)-3-hydroxybutyric acid).<sup>27</sup> Digital filtration may be impractical when residual signals are large, broad, and distorted, as in Figure 8a, but this is not the case here. Such filters can be easily automated to help with the normalisation of data destined for statistical analysis, especially when very low metabolite concentrations are expected. However, the performance of the sequence is such that this is rarely necessary.

It is important, if very high levels of suppression are sought, to optimize the duration and strength of the pulsed field gradients, as well as their ratios. We have found that a ratio of 5.8 between the first and the second gradient pairs produces excellent results when 1 ms long gradient pulses of 28.3 G cm<sup>-1</sup> (first pair) are used. The optimum gradient stabilization delay varies among probes but 0.5 to 1 ms delays are often adequate. It was found that in order to minimize signal distortions the pre-focusing gradient pulses and the first radio-frequency pulse should be separated by at least 1.5 ms,

although this may vary among probes. The number of scans should be a multiple of two, and a minimum of 8 scans should be acquired. Finally, alternating the polarity of the gradient pulses every other scan seems to slightly improve results. Again, the latter is probably probe dependent.

## 4 Conclusions

The present publication presents an efficient and robust, yet easy to set-up, pulse sequence. The pulse sequence deals well with pulse mis-calibrations, radiation damping, chemical exchange, the presence of sample inhomogeneities and significant variations in sample characteristics such as pH, ionic strength, relaxation characteristics and molecular weight. The pulse sequence produces undistorted line shapes and baselines and works well both under automation and in the hands of non-experts. In addition, the new pulse sequence reduces a typical 50 M water signal down to less than 1 mM, a signal attenuation factor suited for the most demanding applications. Other pulse sequences of equal or even better quality can be derived using the principles discussed.

## Acknowledgements

The authors are indebted to the Durham University (UK) solution-state NMR service.

## Notes and references

- 1 R. T. McKay, *Annual Reports on NMR Spectroscopy*, 2009, **66**, 33.
- 2 G. Zheng and W. S. Price, *Progress in Nuclear Magnetic Resonance Spectroscopy*, 2010, **56**, 267.
- 3 J. Wang, X. Zhang, P. Sun, X. Jiang, B. Jiang, C. Cao and M. Liu, *Journal of Magnetic Resonance*, 2010, **206**, 205.
- 4 I. Berregi, J. I. Santos, G. del Campo, J. I. Miranda and J. M. Aizpurua, *Analytica Chimica Acta*, 2003, **486**, 269.
- 5 C. A. Daykin, R. Bro and F. Wulfert, *Metabolomics*, 2012, **8**, S52.
- 6 Y. Du, W. Lan, Z. Ji, X. Zhang, B. Jiang, X. Zhou, C. Li and M. Liu, *Analytical Chemistry*, 2013, **85**, 8601.
- 7 C. A. Lepre, J. M. Moore and J. W. Peng, *Chemical Reviews*, 2004, **104**, 3641.
- 8 B. Lam and A. J. Simpson, *Analyst*, 2008, **133**, 263.
- 9 T. L. Hwang and A. J. Shaka, *Journal of Magnetic Resonance, Series A*, 1995, **2**, 275.
- 10 M. Liu, X. Mao, C. Ye, H. Huang, J. K. Nicholson and J. C. Lindon, *Journal of Magnetic Resonance*, 1998, **132**, 125.
- 11 G. Zheng, A. M. Torres and W. S. Price, *Journal of Magnetic Resonance*, 2008, **194**, 108.
- 12 B. D. Nguyen, X. Meng, K. J. Donovan and A. J. Shaka, *Journal of Magnetic Resonance*, 2007, **184**, 263.
- 13 R. W. Adams, C. M. Holroyd, J. A. Aguilar, M. Nilsson and G. A. Morris, *Chemical Communications*, 2013, **49**, 358.
- 14 T. Parella, P. Adell, F. Sánchez-Ferrando and A. Virgili, *Magnetic Resonance in Chemistry*, 1998, **36**, 245.
- 15 Y. B. Monakhova, H. Schäfer, E. Humpfer, M. Spraul, T. Kuballa and D. W. Lachenmeier, *Magnetic Resonance in Chemistry*, 2011, **49**, 734.

- 16 A. Botana, J. A. Aguilar, M. Nilsson and G. A. Morris, *Journal of Magnetic Resonance*, 2011, **208**, 270.
- 17 K. Takegoshi, K. Ogura, K. Hikichi, *Journal of Magnetic Resonance*, 1989, **84**, 611.
- 18 P. C. M. Van Zijl, C. T. W. Mooned and M. Von Kienlin, *Journal of Magnetic Resonance*, 1990, **89**, 28.
- 19 R. J. Ordidge and I. D. Cresshull, *Journal of Magnetic Resonance*, 1986, **69**, 151.
- 20 M. D. Pelta, G. A. Morris, M. J. Stchedroff and S. J. Hammond, *Magnetic Resonance in Chemistry*, 2002, **40**, S147.
- 21 G. Wider, V. Dötsch and K. Wüthrich, *Journal of Magnetic Resonance, Series A*, 1994, **108**, 255.
- 22 G. A. Morris, H. Barjat and T. J. Home, *Journal of Progress in Nuclear Magnetic Resonance Spectroscopy*, 1997, **31**, 197.
- 23 P. Ebrahimi, M. Nilson, G. A. Morris, H. M. Jensen and S. B. Engelsens, *Journal of Chemometrics*, 2014, **28**, 656.
- 24 R. W. Dykstra, *Journal of Magnetic Resonance*, 1987, **72**, 162.
- 25 M. R. Bendall and D. T. Pegg, *Journal of Magnetic Resonance*, 1985, **63**, 494.
- 26 Y. Lin, N. Lisitza, S. Ahn and W. S. Warren, *Science*, 2000, **290**, 118.
- 27 N. Psychogios, D. D. Hau, J. Peng, A. C. Guo, R. Mandal, S. Bouatra, I. Sinelnikov, R. Krishnamurthy, R. Eisner, B. Gautam, N. Young, J. Xia, C. Knox, E. Dong, P. Huang, Z. Hollander, T. L. Pedersen, S. R. Smith, F. Bamforth, R. Greiner, B. McManus, J. W. Newman, T. Goodfriend and D. S. Wishart, *PLoS ONE*, 2011, **6**, e16957.